Particle states of Lattice QCD

A. S. Kapoyannis[†1] and A. D. Panagiotou[*2]

[1,2]Nuclear and Particle Physics Section, Faculty of Physics, University of Athens, GR-15784 Greece

arXiv:1705.00291v2 [hep-ph] 5 Dec 2017

Abstract

We determine the degeneracy factor and the average particle mass of particles that produce the Lattice QCD pressure and specific entropy at zero baryon chemical potential. The number of states of the gluons and the quarks are found to converge above T =230 MeV to almost constant values, close to the number of states of an ideal Quark-Gluon Phase, while their assigned masses retain high values. The number of states and the average mass of a system containing quarks in interaction with gluons are found to decrease steeply with increase of temperature between $T \sim 150$ and 160 MeV, a region contained within the region of the chiral transition. The minimum value of the number of states within this temperature interval indicates that the states are of hadronic nature.

1 Introduction

The results from heavy ion collisions at RHIC and LHC suggest that the quark-gluon state formed is a strongly interacting one. The fact that the LHC at the highest energy of $\sqrt{s}_{NN}$= 5.02 TeV produced collision temperatures of more than 300 MeV, pushed the "ideal state" of non-interacting entities to enormous temperatures.

Hagedorn, a pioneer in the investigation of the hadronic properties, had suggested that a strongly interacting system can be equivalently described as a system of non-interacting entities with corresponding masses. In this picture the interaction is hidden in "particle" states [1]. Recently, a quasi-particle using massive gluon states for the thermodynamic description of non-abelian interacting gluon plasma has been developed [2].

Given the above, we may reasonably ask if it is possible to find "particle" massive states, which could equivalently describe the existing, precise results of lattice calculations for the equation of state of QCD matter.

In this work we study this possibility. In section 2 we review the Lattice calculations which are the input of our calculations. In section 3 we describe the method we will use and apply it to a simple, instructive model. In section 4 we present our results firstly on the Hadron Resonance Gas (HRG) and then on the QCD system. Specifically, we fit the lattice pressure and specific entropy with a model of two parameters, the number of "degenerate" states and the average mass and explore the variation of these two parameters with temperature. Finally, we discuss our conclusions in section 5.

[†]email: akapog@phys.uoa.gr

[*]email: apanagio@phys.uoa.gr

2 Lattice calculations

Lattice calculations have been carried out for (2+1) flavor QCD, i.e. for two light and one strange quark state at vanishing baryon chemical potential [3]. In Figure 2 of [3], the authors present their estimation of suitably normalised pressure P, entropy density s and energy density ϵ, of a QCD system in the temperature range 130-400 MeV. The transition temperature is taken to be $T_c \simeq 154$ MeV, while the smooth curves suggest the existence of a crossover region. In Table I of [3] the numerical values of the previous quantities with their corresponding errors are recorded. Also, in eq. (16) of [3] a parametrisation is given which fits quite well the numerical values of the pressure curve. This parametrisation agrees with the lattice data well above 400 MeV. The curves approach the corresponding Hadron Resonance Gas (HRG) curves for temperatures $T \leq 180$ MeV. This is expected since HRG models [4] describe well the freeze- out data from the heavy-ion collisions.

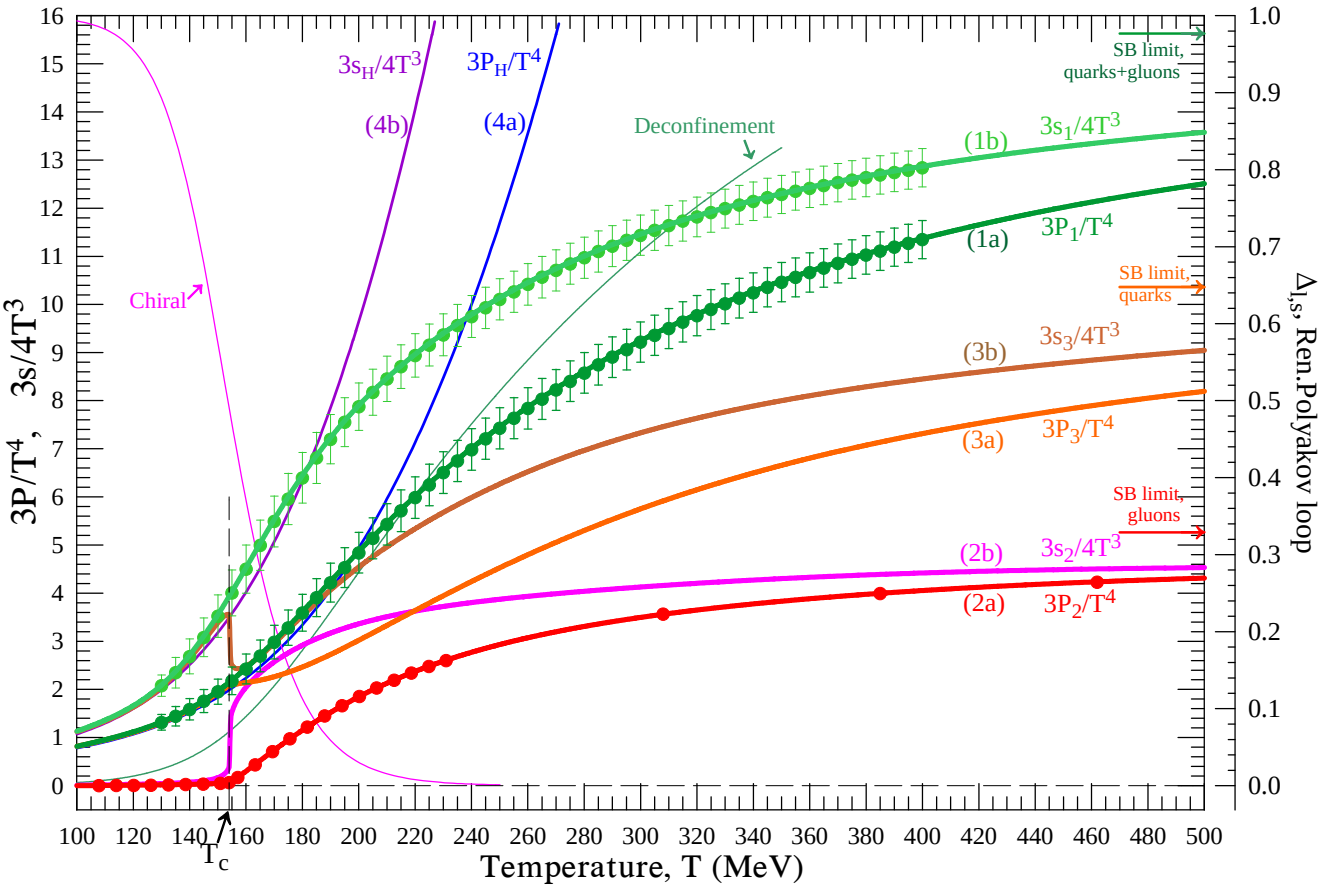


Figure 1: Calculation of the normalised Pressure, P (curves a) and entropy density, s (curves b). Lattice calculation for (2+1) flavour QCD correspond to lines 1, lattice calculations for the SU(3) gauge field to lines 2 and lines 3 to the result of subtracting the values of lines 2 from the corresponding values of lines 1. Estimation for the Hadron Resonance Gas (HRG) corresponds to lines 4. Also shown are the corresponding non-interacting (SB) limits and the lattice estimation of the order parameters of the chiral transition and deconfinement (corresponding to the far right vertical axis).

The system described by the full QCD Lagrangian including the fermionic and gluonic fields and all the interactions among them will be referred in this paper as system 1. We will use the corresponding Lattice calculations for this system, which we depict in curves 1 of Figure 1. In curve (1a) of Figure 1 we depict the numerical calculations for the normalised pressure $\frac{3P_1}{T^4}$, as well as the parameterisation of [3]. In curve (1b) the numerical calculations for the normalised specific

entropy $\frac{3s_1}{4T^3}$ are shown. Assuming that the pressure P does not depend on the system volume, the corresponding curve is found from the parametrisation of curve (1a), since

$$s = \frac{dP}{dT} \tag{1}$$

In Figure 1 we also show our calculations of the curves of normalised pressure and entropy of the Hadron Resonance Gas (HRG) model (curves (4a) and (4b), respectively). The calculations have been carried out in the Boltzmann approximation, since in this temperature range the effect of the inclusion of the correct statistics is negligible at these conditions.

Lattice calculations for the gauge field of QCD have been carried out in [5], as well. In Table 1 of this work the pressure as a function of temperature is recorded for a wide range of values ($0.7 \leq \frac{T}{T_c} \leq 1000$). The system described by the Lagrangian including only the gluonic fields and the interactions only among them will be referred in this paper as system 2. We will use the corresponding Lattice calculations for this system, which we depict in curves 2 of Figure 1. We apply again $T_c = 154$ MeV and record these values as solid circles in curve (2a) of Figure 1, which represents the relative normalised pressure $\frac{3P_2}{T^4}$. In order to be able to work with these values we need a continuous and derivable function. Thus, we apply a fit on the values. Since we cannot find a suitable function for the whole temperature range, we use for $T \leq T_c$ the function

$$P_2(T) = a_1 + a_2 T + a_3 \ln(a_4 + a_5 T) \tag{2}$$

For $T \geq T_c$ we find as a suitable function to fit the data the following:

$$P_2(T) = b_1 \left\{1 - exp\left[-b_2(x - b_3)^{b_4}\right]\right\} + b_5 \left\{1 - exp\left[-b_6(T - T_c)^{b_7}\right]\right\} \tag{3}$$

The phase transition for the pure SU(3) gauge system is of first order. This results in discontinuity in the first derivative of pressure and in the entropy density. This discontinuity can be problematic in method 1 we will describe in the next section, since the method cannot be applied around the critical temperature. In order to avoid this discontinuity between the functions (2) and (3), we interpolate with a polynomial of 5^{th} grade in the temperature range $T_c \leq T \leq T_c + 0.5MeV$:

$$P_2(T) = c_1 + c_2 T + c_3 T^2 + c_4 T^3 + c_5 T^4 + c_6 T^5 \tag{4}$$

However, we have to note that our calculations in this small temperature range where we impose the interpolation will have to be taken cautiously into account in the sense they may produce continuities where discontinuities exist. We impose the constraint that the polynomial will produce continuity up to 2^{nd} derivative at the boundary values. The values of the parameters of our fitting functions are listed in Table 1. We prefer to use eqs. (2)-(4) instead of the functions listed in [5] because the latter are valid only at certain temperature regions, while we need a function valid at the whole temperature region on which we work.

Line (2b) in Figure 1 represents the corresponding normalised entropy density, $\frac{3s_2}{4T^3}$, as it is calculated from eq. (1), using eqs. (2)-(4).

We will also use as input in our calculations the pressure and entropy density which result from subtracting the corresponding quantities of system 2 from those of system 1:

$$P_3 = P_1 - P_2 \ \ , \ s_3 = s_1 - s_2 \ . \tag{5}$$

Equations (5) describe a system of fermionic fields in interaction with gluons which will be referred to in this work as system 3. This system differs from the total system 1 in the exclusion of the contribution of the gluons (system 2). This separation cannot in principle be made in an interacting theory. However, this separation is useful in the sense that, as will become evident in section 4, at

Symbol/Value	Symbol/Value	Symbol/Value
a_1 =0.06398	b_1 =0.81546	c_1 =-1125870000
a_2 =0.00001	b_2 =0.00279	c_2 =36430317
a_3 =-0.00692	b_3 =147.3457	c_3 =-471516.11
a_4 =32351.103	b_4 =1.15198	c_4 =3051.3982
a_5 =-206.61058	b_5 =0.69596	c_5 =-9.8734740
	b_6 =0.01106	c_6 =0.012779088
	b_7 =1.15973	

Table 1: The parameters used in the fitting functions of the SU(3) pressure.

temperatures $T > 230$ MeV system 3 leads to a system containing only quark degrees of freedom, while system 2 to a system with only gluonic degrees. Also, at temperatures below the critical one ($T < 154$ MeV) system 3 converges to system 1, acquiring the hadronic degrees of freedom, while system 1 results to negligible contribution to pressure and entropy density (Figure 1). The curves corresponding to system 3 are curve (3a) for the normalised quark pressure and curve (3b) for the normalised entropy density, $\frac{3s_3}{4T^3}$.

In Figure 1 we depict with horizontal lines the Stefan-Boltzmann (SB) limit for massless and non-interacting particles. For gluons (bosons) the pressure is given by

$$\frac{P_g}{T^4} = \frac{\pi^2}{90} g_G \equiv \frac{\pi^2}{90} g_s g_c = \frac{\pi^2}{90} 2 \cdot 8 = \frac{\pi^2}{90} 16 \ , \tag{6}$$

where $g_G = 16$ is the total number of states of gluons due to their spin, $g_s = 2$ and colour, $g_c = 8$. For the quarks (fermions) the pressure is given by

$$\frac{P_q}{T^4} = \frac{7}{8}\frac{\pi^2}{90} g_Q \equiv \frac{7}{8}\frac{\pi^2}{90} g_s g_c g_f g_{an} = \frac{7}{8}\frac{\pi^2}{90} 2 \cdot 3 \cdot 3 \cdot 2 = \frac{7}{8}\frac{\pi^2}{90} 36 \ , \tag{7}$$

where $g_Q = 36$ is the total number of states of quarks due to their spin, $g_s = 2$, colour, $g_c = 3$, flavours which are present in (2+1) flavour QCD, $g_f = 3$ and the presence of quarks and anti-quarks, $g_{an} = 2$. Normalising the entropy density as $\frac{3s}{4T^3}$ we get the same SB limit as the pressure $\frac{3P}{T^4}$.

In [6] (Figure 4, Table 3) there is calculation of $\Delta_{l,s}$ as a function of temperature, a quantity related to the chiral condensate, which can be taken as an indicator for the remnant of the chiral transition, since it shows abrupt change. Also, in [6] (Figure 3, Table 3) there is an estimation of the renormalised Polyakov loop, the order parameter of the deconfinement phase transition of QCD in the pure gauge sector. We depict in Figure 1 our fits to the values of these two quantities listed in [6].

3 Method

We address the question which single particle state would have the same pressure with the lattice QCD calculations at a particular temperature. For this reason we assume that the partition function of this particle state at vanishing baryon chemical potential will be

$$\ln Z_f(V, T; g_t, \langle m \rangle) = \frac{VT}{2\pi^2} g_t \langle m \rangle^2 K_2 \left(\frac{\langle m \rangle}{T} \right) \ . \tag{8}$$

We use the above partition function, which is in the Boltzmann approximation, in the absence of knowledge whether the particles of our system are fermions, bosons or a mixture of both. Also,

the correct statistics are not expected to produce high differences at the temperatures considered. The pressure and entropy density related to (8) will then be

$$P_f(T; g_t, \langle m \rangle) = \frac{T^2}{2\pi^2} g_t \langle m \rangle^2 K_2 \left(\frac{\langle m \rangle}{T} \right) , \tag{9}$$

$$s_f(T; g_t, \langle m \rangle) = \frac{g_t \langle m \rangle^2}{2\pi^2} \left\{ 2T K_2 \left(\frac{\langle m \rangle}{T} \right) + \frac{\langle m \rangle}{2} \left[K_1 \left(\frac{\langle m \rangle}{T} \right) + K_3 \left(\frac{\langle m \rangle}{T} \right) \right] \right\} . \tag{10}$$

The problem is, henceforth, limited to determining the quantity $\langle m \rangle$, which corresponds to the mass of a particle, as well as the degeneracy factor g_t, which is the total number of states that corresponds to this particle (due to its spin, colour, etc.). To address the problem we have developed two methods.

In method "1" we consider a part of the Lattice pressure curve $P_L(T)$ which extends in the temperature interval $(T - \Delta T, T + \Delta T)$ around a central value T. We divide the interval in $N - 1$ equal parts, with N being rather large (we use for all calculations in this paper $N = 101$). The corresponding temperature values are T_i, $i = 1, N$. Then we determine g_t and $\langle m \rangle$ by minimizing the quantity

$$\chi^2 = \sum_{i=1}^{N} \frac{1}{\sigma_i^2} \left[P_L(T_i) - P_f(T_i; g_t, \langle m \rangle) \right]^2 , \tag{11}$$

The determined values g_t and $\langle m \rangle$ can then be assigned to the central temperature value T. In the definition of χ^2, σ_i are errors in the values $P_L(T_i)$. Since all the points i should have the same weight in the calculation these errors should be equal for the same central temperature T. However, to compare values of χ^2 at different temperatures T we should consider the fact that pressure rises rapidly with T. Consequently, it is expected that the deviations between the pressure P_L and the fitting pressure P_f to increase with the rise of T, if we use constant values for σ_i for all T. In order to compensate this fact and avoid the systematic growth of χ^2 with temperature we use for the errors the function

$$\sigma(T) = f(T) = T^4 , \tag{12}$$

which has also been used extensively for the normalisation of pressure. We note, though, that the exact position of the maxima of χ^2 will depend on the function used in (12), while this choice will cause no effect on the determination of the parameters g_t and $\langle m \rangle$, as it is evident from eq. (11).

In method "2" we use the values of the Lattice pressure $P_L(T)$ and the Lattice energy density $s_L(T)$ at a specific temperature T. Then we solve the following set of two equations to determine g_t and $\langle m \rangle$ which correspond to the specific value of T:

$$P_L(T) = P_f(T; g_t, \langle m \rangle) \quad , \quad s_L(T) = s_f(T; g_t, \langle m \rangle) \tag{13}$$

The choice of the two thermodynamic functions $P_L(T)$ and $s_L(T)$, which we use as input in method 2, is not unique. Let us suppose, on the event of use of the pair $P_L(T)$ and $s_L(T)$, that we want to fit another thermodynamic quantity r_L which can be expressed as function of the used two quantities,

$$r_L(T) = F(P_L(T), s_L(T)) . \tag{14}$$

We want to fit the quantity r_L with the same parameters g_t and $\langle m \rangle$. So

$$r_L(T) = r_f(T; g_t, \langle m \rangle) , \tag{15}$$

where r_f is the fitting function which corresponds to the quantity r and which is calculated from the partition function for a system with one particle species (like eqs. (9),(10)). Combining eqs. (14), (15) and (13), we find that the following equation has to hold for every temperature T:

$$r_f(T; g_t, \langle m \rangle) = F(P_f(T; g_t, \langle m \rangle), s_f(T; g_t, \langle m \rangle)) . \tag{16}$$

Now if g_{ta}, $\langle m \rangle_a$ is the solution of eqs. (13) for the parameters for a specific temperature T_a, the quantity r_L will be at the same temperature:

$$r_{La} \equiv r_L(T_a) = F(P_L(T_a), s_L(T_a)) = F(P_f(T; g_{ta}, \langle m \rangle_a), s_f(T; g_{ta}, \langle m \rangle_a)) = r_f(T; g_{ta}, \langle m \rangle_a) \quad (17)$$

The last equation verifies that the parameters g_t and $\langle m \rangle$ that were found to fit the pressure and entropy density at a certain temperature will also fit exactly the quantity r_L. If the partition function does not depend on the system volume and if we work at vanishing chemical potential, we can use as function r_L the entropy density ε_L, since:

$$\varepsilon_L(T) = -P_L(T) + T s_L(T), \quad (18)$$

or the trace anomaly, used extensively by lattice practitioners, since

$$\Theta^{\mu\mu}_L(T) = \varepsilon(T) - 3P_L(T) = T s_L(T) - 4P_L(T). \quad (19)$$

One can equivalently use in method 2 any two of a set of thermodynamic quantities that can be expressed as a function of each other to determine the two parameters g_t and $\langle m \rangle$.

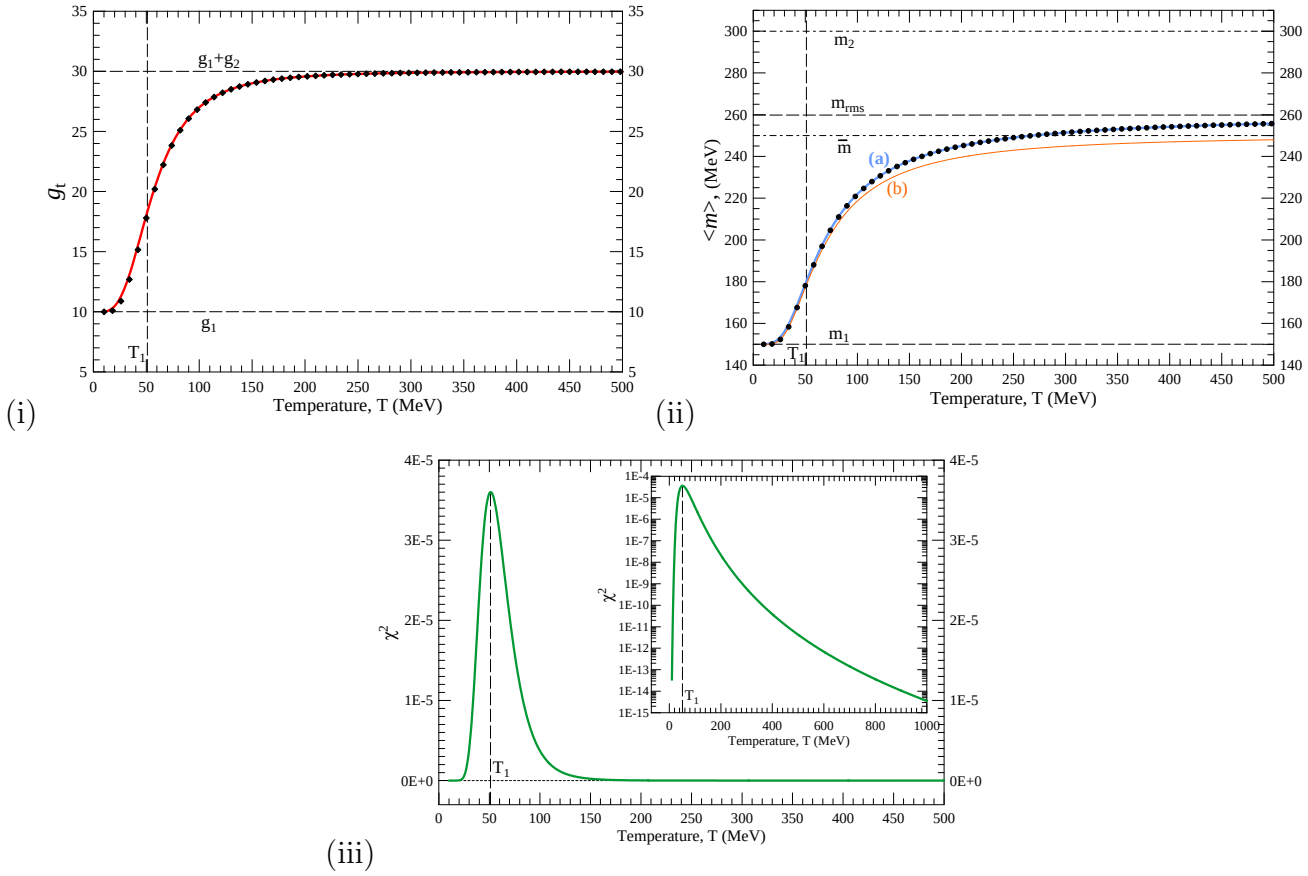


Figure 2: Analysis of the partition function of a system with two particle species with degeneracy factors $g_1 = 10$ and $g_2 = 20$ and mass $m_1 = 150$ MeV and $m_2 = 300$ MeV, respectively. (i) g_t as a function of temperature with method 1 (continuous line) and method 2 (solid squares). (ii) $\langle m \rangle$ as a function of temperature (curve (a)) with method 1 (continuous line) and method 2 (solid circles). Curve (b) represents an approximation valid for low temperatures. (iii) The value of χ^2 as a function of temperature for method 1.

Comparing the results from the two methods it is deduced that they are in general equivalent. This is expected since in method 1 we fit the shape of a segment of the pressure curve. By taking

a lot of points on this part and requiring these points to be fitted by our theoretical pressure function we impose the constraint not only to fit the specific value of $P_L(T)$ at T but also the higher derivatives of the function $P_L(T)$ at T. In method 2, according to eqs. (13) we fix our theoretical functions to fit the Lattice pressure and its first derivative (entropy density). Thus, we expect the outcome from the two methods to be approximately the same.

However, method 1 gives us the additional opportunity to calculate the value of χ^2. This value can be taken as a measure of how well function (9) fits the Lattice pressure. On the other hand, in method 1 the results may depend on the value of the temperature interval ΔT. These issues will be discussed in the following section.

Additionally, since the pressure can be expressed as an integral of the entropy density we could start by fitting in method 1 a segment of the curve of the entropy density. Thus, the choice of the pressure in method 1 is not unique.

We shall end this section by performing some "toy" fits that will enable us to have insight on the meaning of the parameters g_t and $\langle m \rangle$. In the first case we consider a system composed of one boltzmannian particle with degeneracy factor g_1 and mass m_1. The relevant pressure is then

$$P_a(T) = \frac{T^2}{2\pi^2} g_1 m_1^2 K_2\left(\frac{m_1}{T}\right) \ . \tag{20}$$

If we perform method 1 or method 2 we find $g_t = g_1$ and $\langle m \rangle = m_1$. So in this case g_t can be identified as the number of the states of the particle and $\langle m \rangle$ as the mass of this particle.

We then consider a system composed of two particles with pressure

$$P_b(T) = \frac{T^2}{2\pi^2} g_1 m_1^2 K_2\left(\frac{m_1}{T}\right) + \frac{T^2}{2\pi^2} g_2 m_2^2 K_2\left(\frac{m_2}{T}\right) \ . \tag{21}$$

In figures 2 we present the results for g_t (fig. (i)) and $\langle m \rangle$ (fig. (ii)) as a function of temperature. We will determine the low and high temperature limits of these two entities. The modified Bessel functions of the 2nd kind can be approximated for large arguments (low temperatures) as

$$K_2(z) \underset{z\to\infty}{\longrightarrow} \sqrt{\frac{\pi}{2z}} e^{-z} \Rightarrow K_2\left(\frac{m}{T}\right) \underset{T\to 0}{\longrightarrow} \sqrt{\frac{\pi}{2}\frac{T}{m}} e^{-m/T} \ . \tag{22}$$

From this we get

$$P_b(T) = P_f(T; g_t, \langle m \rangle) \underset{T\to 0}{\Rightarrow} g_1 m_1^2 \sqrt{\frac{\pi}{2}\frac{T}{m_1}} e^{-m_1/T} + g_2 m_2^2 \sqrt{\frac{\pi}{2}\frac{T}{m_2}} e^{-m_2/T} = g_t \langle m \rangle^2 \sqrt{\frac{\pi}{2}\frac{T}{\langle m \rangle}} e^{-\langle m \rangle/T} \Rightarrow$$

$$g_1 m_1^{3/2} e^{(\langle m \rangle - m_1)/T} + g_2 m_2^{3/2} e^{(\langle m \rangle - m_2)/T} = g_t \langle m \rangle^{3/2} \tag{23}$$

For eq. (23) to be valid, the exponential with the greater exponent has to be eliminated. Since $m_1 < m_2$, this requirement leads to

$$\langle m \rangle \underset{T\to 0}{\longrightarrow} m_1 \tag{24}$$

Automatically, the other exponential acquires negative exponent and tends to zero. Thus

$$g_t \underset{T\to 0}{\longrightarrow} g_1 \tag{25}$$

Eqs. (24),(25) prove what is evident from figures 2(i)-(ii). For low temperatures the system can effectively be described as a system containing only states with the lowest mass m_1. However, as the temperature rises, the states with mass m_2 begin to "unlock", i.e. affecting the system. To find the effective description of our system for large temperatures we need an approximation of

the $m^2K_2(m/T)$ function for small arguments that will depend on m. Thus we use the following approximation of the modified Bessel functions of the 2nd kind for small arguments

$$K_2(z) = \frac{z}{4}[K_3(z) - K_1(z)] \underset{z\to 0}{\longrightarrow} 2z^{-2} - \frac{1}{4} \Rightarrow m^2 K_2\left(\frac{m}{T}\right) \underset{T\to\infty}{\longrightarrow} 2T^2 - \frac{m^2}{4} \ . \tag{26}$$

Last equation leads to

$$P_b(T) = P_f(T; g_t, \langle m\rangle) \underset{T\to\infty}{\Rightarrow} g_1\left(2T^2 - \frac{m_1^2}{4}\right) + g_2\left(2T^2 - \frac{m_2^2}{4}\right) = g_t\left(2T^2 - \frac{\langle m\rangle^2}{4}\right) \Rightarrow$$

$$2(g_1 + g_2 - g_t)T^2 - \frac{1}{4}(g_1 m_1^2 + g_2 m_2^2 - g_t \langle m\rangle^2) = 0 \tag{27}$$

Demanding eq. (27) to be valid, we find that g_t tends to the sum of the number of states of all (two) particles, while the limit of $\langle m\rangle$ becomes the square root of the mean value of the square of the masses:

$$g_t \underset{T\to\infty}{\longrightarrow} g_1 + g_2 \tag{28}$$

$$\langle m\rangle \underset{T\to\infty}{\longrightarrow} m_{rms} = \sqrt{\frac{g_1 m_1^2 + g_2 m_2^2}{g_1 + g_2}} \ . \tag{29}$$

Eq. (28) enables us to identify g_t as the "total" number of particle states, while eq. (29) suggests that $\langle m\rangle$ can be identified as the "mean" mass of particle states. Also, another important fact from eq. (27) is that g_t is connected to the leading temperature term T^2. This forces g_t to approach to high temperature limit (28) more rapidly than $\langle m\rangle$ approaches the relevant limit (29). This attribute is evident by comparing Figures 2(i)-(ii).

The mass $\langle m\rangle$ can also be approximated in a wide temperature range, which are not high, by the average of the two masses weighted by their contribution to the pressure (curve (b) of figure 2(ii)):

$$\bar{m} = \frac{m_1[g_1 m_1^2 K_2\left(\frac{m_1}{T}\right)] + m_2[g_2 m_2^2 K_2\left(\frac{m_2}{T}\right)]}{g_1 m_1^2 K_2\left(\frac{m_1}{T}\right) + g_2 m_2^2 K_2\left(\frac{m_2}{T}\right)} \ . \tag{30}$$

The high temperature limit of (30) with the use of only the leading term of (26) is found to be:

$$\bar{m} \simeq \frac{g_1 m_1 + g_2 m_2}{g_1 + g_2} \ . \tag{31}$$

Figures 2(i)-(ii) also show the equivalence of the two methods. In Fig. 2(iii) we show the variation of χ^2 as function of temperature. It is evident from the low value of χ^2 that our description with eq. (8) is valid throughout the whole temperature range. The value of χ^2, though, can offer us additional information. In fig. 2 we depict with vertical line the position at temperature T_1 of the maximum value of χ^2. This vertical line is depicted in figures 2(i)-(ii), as well. The maximisation of χ^2 suggests a relatively worse description with the used parameters at T_1 compared with the relatively better description at lower and higher temperatures. At low temperatures the description is carried out by $g_t = g_1$ and $\langle m\rangle = m_1$, while at high temperatures by $g_t = g_1 + g_2$ and $\langle m\rangle = m_{rms}$. Both of these two descriptions are connected with relatively lower value of χ^2. Also, T_1 coincides with the temperature at which g_t or $\langle m\rangle$ exhibits great variation (with respect to the temperature). Thus, the temperatures at which the local maximum values of χ^2 are located signal transition regions from one effective description, with one set of values of g_t and $\langle m\rangle$, to another, with different set of values of g_t and $\langle m\rangle$.

4 Results

We will apply the methods presented in the previous section firstly to the Hadron Resonance Gas (HRG). The model we use does not include volume corrections, nor other interaction among the hadrons. It is interesting to analyse HRG because it serves as the lower limit of lattice QCD. As it is evident from Figure 1 the HRG pressure and entropy density remains close to the corresponding lattice calculations even above critical temperature and up to about 190 MeV. Also, the HRG model we will use is a group of particle states with three flavours and masses up to about 2400 MeV. As such, it will enable us to verify and extend our conclusions of the two particle states toy model we described in the previous section. Lastly, the HRG model will be utilised to contrast the behaviour of the QCD system. The particles are non-interacting and, thus, exhibit no phase transition. Also, the particle masses remain unchanged in the entire temperature range.

In Figure 3(i) we show the pressure and the energy density of the HRG model in the Boltzmann approximation (continuous lines), as well as, the results with the correct statistics, Bose-Einstein or Fermi-Dirac for every particle (points). Up to $T \simeq 500$ MeV, a temperature range that will interest us in the following, the discrepancies between the approximation and the correct statistics are negligible.

In Figure 3(ii) we present the calculation of the total number of states g_t for the HRG as function of temperature with method 1 (continuous lines) and method 2 (points). The lower temperature limit of g_t is $g_\pi = 3$, which is the number of states of the lighter hadrons, i.e. the pions (π^0, π^+ and π^-). The high temperature limit of g_t is checked to be the one corresponding to equation (28), which for the N particle species we have used is:

$$g_t = \sum_{i=1}^{N} g_i = 1639. \tag{32}$$

In Figure 3(iii) we present the calculation of the average mass $\langle m \rangle$ for the HRG as function of temperature with method 1 (solid lines) and method 2 (points). The lower temperature limit of $\langle m \rangle$ is the mass of the lighter hadron, i.e. the pion. The higher temperature limit of $\langle m \rangle$ is checked to be the corresponding to eq. (29), which for the N particle species we have used is:

$$m_{rms} = \sqrt{\frac{\sum_{i=1}^{N} g_i m_i^2}{\sum_{i=1}^{N} g_i}} \simeq 1873.65 \text{ MeV}. \tag{33}$$

In Figure 3(iv) we show the value of χ^2 of method 1. The temperature T_1 corresponds to the higher value of χ^2. Comparing Figure 3(iv) with Fig. 2(iii) we find that χ^2 develops a maximum that is "broader" than the two particle model of the previous section. This is caused by the large number of resonances that exist in the HRG model, which are scattered to the whole mass range from the pion mass up to 2400 MeV.

We proceed by analysing the Lattice results presented in Fig. 1. We limit our analysis in temperatures up to 500 MeV, since the calculations for (2+1) flavour QCD are limited up to 400 MeV (see Fig. 1), above which only the extrapolation function is available [3]. In Figure 4 we present our calculations for the total number of states g_t and in Figure 5 the calculations for the average mass $\langle m \rangle$. These calculations have been carried out through method 1. Curves (1) correspond to system 1, curves (2) to system 2 and curves (3) to system 3. We, also, present the line corresponding to the HRG (curves (4)). It is seen that the HRG is the low temperature limit of systems 1 and 3, something expected since at low temperatures the system exists in the form of hadrons.

As temperature rises the curves begin to deviate from the HRG curves. The total system reaches a maximum in g_t and $\langle m \rangle$ and then it begins to decrease. System 3 after reaching a local maximum,

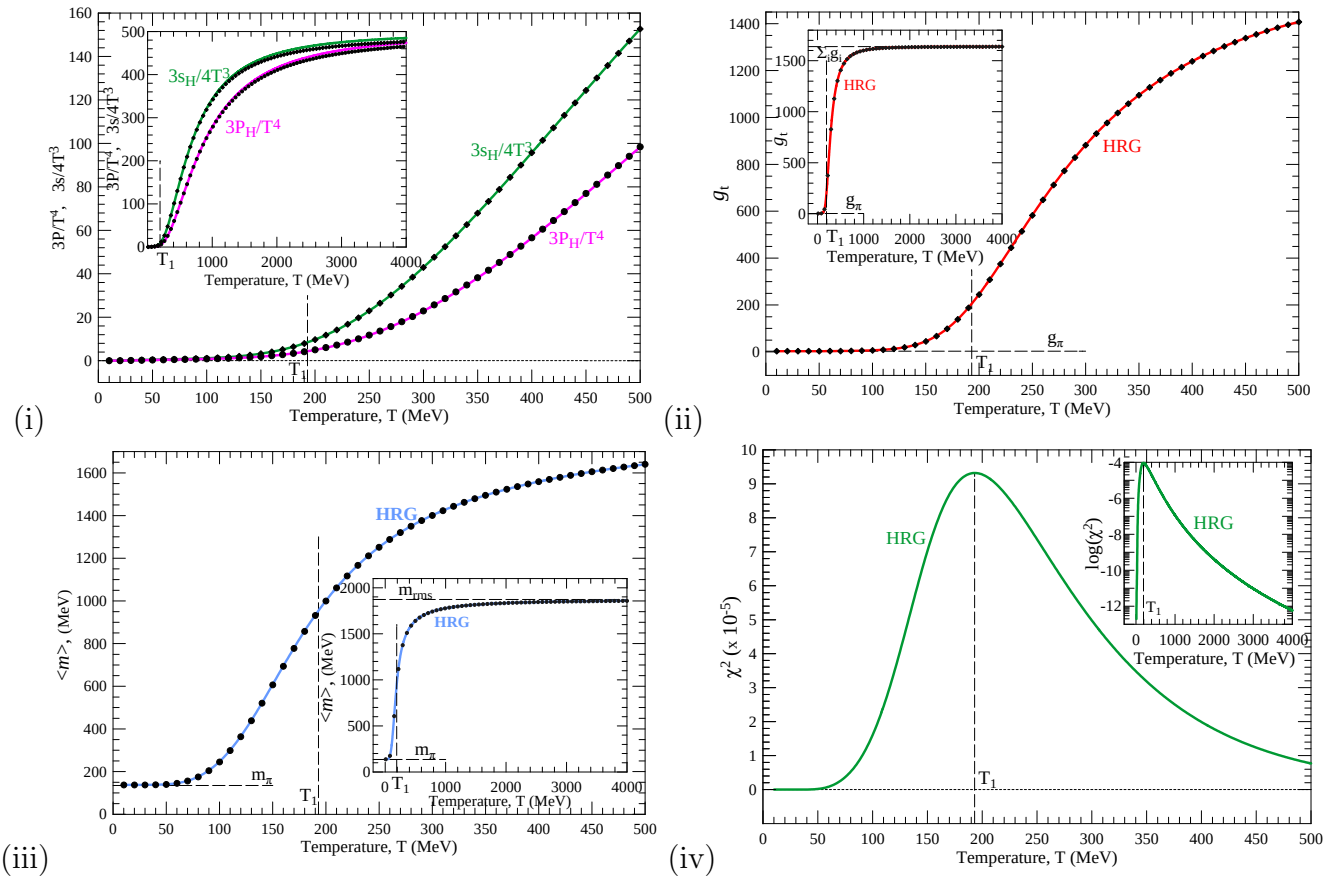


Figure 3: Analysis of the Hadron Resonance Gas (HRG). (i) The normalised pressure, P_H and entropy density, s_H, of the system in the Boltzmann approximation (lines) and with the correct statistics (Bose or Fermi) for every particle (points). The deviations between the two sets of statistics appear in high temperatures, $T \geq 1000$ MeV, where, after all, the HRG is not valid. (ii) g_t as a function of temperature with method 1 (continuous line) and method 2 (solid squares). (iii) $\langle m \rangle$ as a function of temperature with method 1 (continuous line) and method 2 (solid circles). (iv) The value of χ^2 as a function of temperature for method 1.

it decreases abruptly to arrive at a local minimum. Then it increases again to a local maximum and finally it stabilizes. These variations of g_t and $\langle m \rangle$ occur in the temperature range of the chiral transition. This behaviour is contrasted to a system with constant particle states. Such a system would have an effective description with g_t and $\langle m \rangle$ always increasing when temperature increases. For example we can see the behaviour of the HRG in Figures 3 (ii) and (iii). The decrease of the number of states of systems 1 and 3 suggests that the QCD system, as it is heated, it is driven to a gradual reduction of available states. The decrease of $\langle m \rangle$, at certain temperature ranges, indicate that the average mass of these states decreases, also. If the separation of the whole system into pure SU(3) sector and the remaining quark-gluon interacting system is approximately correct in the temperature range 154-230 MeV, then an important conclusion can be drawn. The degrees of freedom of the quark-gluon interacting system 3 drops to about 10. Then, this value cannot correspond to quark (coloured) degrees of freedom. The relevant value for the 3 flavours of quarks are 36. Even if we omit the heavy strange quark (on the assumption that its degrees of freedom will "unlock" at a greater temperature) the value for the remaining quarks cannot be less than 24 (in $2+1$ flavour QCD, u and d quarks are considered almost identical). As it is evident from Fig. 2(i), in a model with two particle species, the effective number of states of the whole system can never be less than the number of states of the lighter particle species. Consequently, the degrees of freedom of about 10, just above T_c, can only correspond to hadrons. So it is deduced that, at the critical

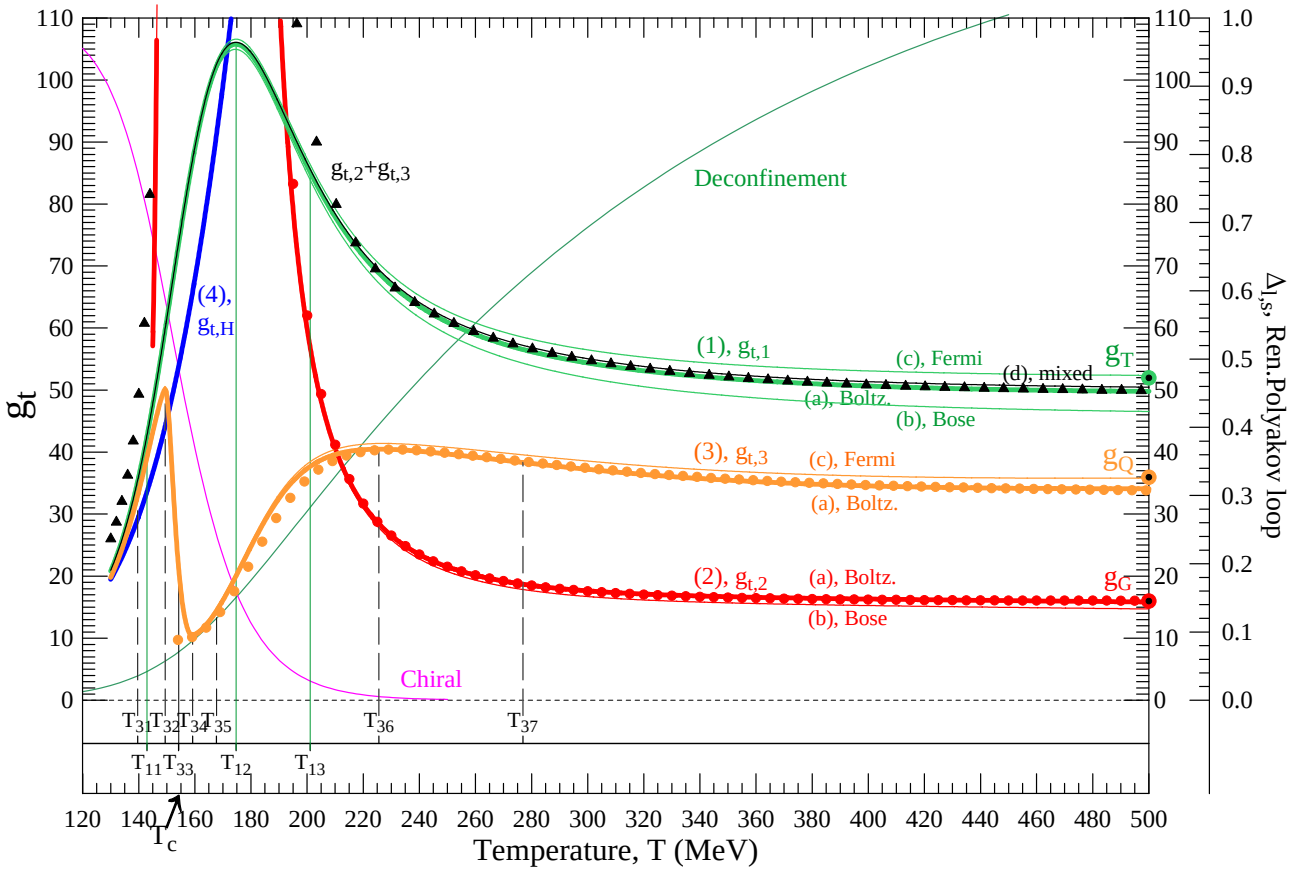


Figure 4: The number of states g_t calculated through method 1 with $\Delta T = 5$ MeV. Curves (1), $g_{t,1}$, correspond to system 1, curves (2), $g_{t,2}$, to system 2, curves (3), $g_{t,3}$, to system 3 and curve (4), $g_{t,H}$, to HRG. Thick lines (a) are calculated with the Boltzmann approximation, lines (b) with Bose statistics, lines (c) with Fermi statistics and thin dark line (d) to a system composed of $\frac{16}{52}$ bosons and of $\frac{36}{52}$ fermions. The solid circles correspond to the number of states of an ideal system containing gluons ($g_G = 16$), quarks ($g_Q = 36$) or gluons and quarks ($g_T = 52$). Solid triangles are the sum $g_{t,2} + g_{t,3}$ of lines (2a) and (3a) and are compared with line (1a). The order parameters of the chiral transition and deconfinement are shown, as in Fig. 1. The shown characteristic temperatures $T_{31...36}$, $T_{11...13}$ are defined below in Fig. 6 and Table 2. $T_c = 154$ MeV, is the critical temperature. With solid rectangles we present the calculations of g_t in the Boltzmann approximation for systems 2 and 3 carried out with the Lattice results from [7].

temperature, the QCD system undergoes a drastic reduction of the hadronic degrees of freedom, possibly a reduction of the available resonances for the hadronic families.

System 2 exhibits a very steep increase as the critical temperature T_c is approached from below. Above T_c the increase is turned to a very steep descend.

At temperatures greater than ~ 250 MeV, which is approximately the temperature where the chiral transition is completed, the number of states of all systems begins to approach an almost constant value. This suggests that the states of the system gradually cease to change. It is remarkable that the results of our fit reveals that the number states of system 2, $g_{t,2}$, tends to the value $g_G = 16$ of eq. (6) and the number states of system 3, $g_{t,3}$, tends to the value $g_Q = 36$ of eq. (7). As a result the total system also tends to the value $g_T = g_G + g_Q = 52$ which is the total number of states of gluons and quarks. The values of g_G, g_Q and g_T are presented at the far right end of Figure 4 as solid circles. Figure 5 shows that the average mass $\langle m \rangle$ does not undergo great changes above ~ 230 MeV. The average mass of quarks, even at $T = 500$ MeV, remains high and is equal to $\simeq 540$ MeV. All these findings are consistent with a description where, above

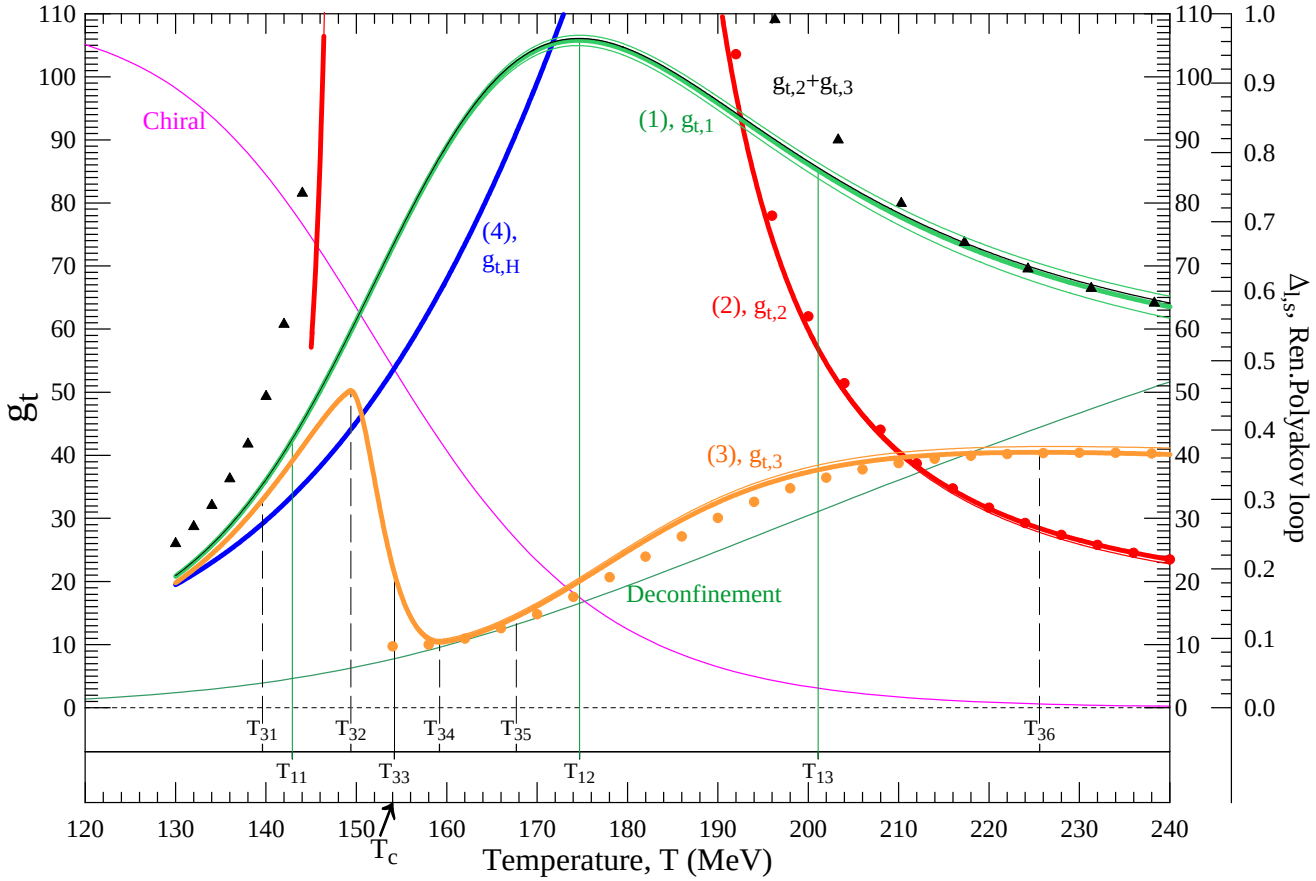


Figure 4a: Fig. 4 focused on the temperature range 120-240 MeV.

$T \simeq 250$ MeV, colour states are present and their number is already locked to their corresponding high temperature limit. However, the system is still strongly interacting. This is indicated by the large value of average mass, which still remains far from the zero value of the SB limit.

The curves (a) of Figs. 4 and 5 are calculated in the Boltzmann approximation (eq. (8)). To check the validity of these calculations we also perform calculations under the assumption that the system is composed of fermions or bosons. For this task we use as fitting partition function the following:

$$\ln Z_{f,BF}(V,T;g_t,\langle m\rangle,\alpha) = \frac{V}{6\pi^2 T} g_t \cdot \int_0^\infty dp \frac{p^4}{\sqrt{p^2+\langle m\rangle^2}} \left[\exp\left(\frac{\sqrt{p^2+\langle m\rangle^2}}{T}\right)+\alpha\right]^{-1}, \quad (34)$$

where $\alpha = -1(+1)$ for bosons(fermions). The results with the Bose statistics are represented by curves (b) and those with the Fermi statistics are represented by curves (c). Since we know system 2 consists of bosons we present only a fit with the Bose statistics. For system 3 we know that it consists of fermions at high temperatures. This system for low temperatures consists of hadrons, a mixture of fermions and bosons. However, at low temperatures all the statistics converge to the same results. For these reasons we present only a fit with the Fermi statistics for system 3. For system 1 we present both statistics, as well as the result of a "mixed" fitting function:

$$\ln Z_{f,m}(V,T;g_t,\langle m\rangle) = \frac{16}{52}\ln Z_{f,BF}(V,T;g_t,\langle m\rangle,-1) + \frac{36}{52}\ln Z_{f,BF}(V,T;g_t,\langle m\rangle,+1) \quad (35)$$

All the results, with all types of statistics, are found to coincide for $T \leq 200$ MeV. At $T \simeq 500$ MeV the deviation between the Boltzmann approximation and the Bose/Fermi statistics is at most

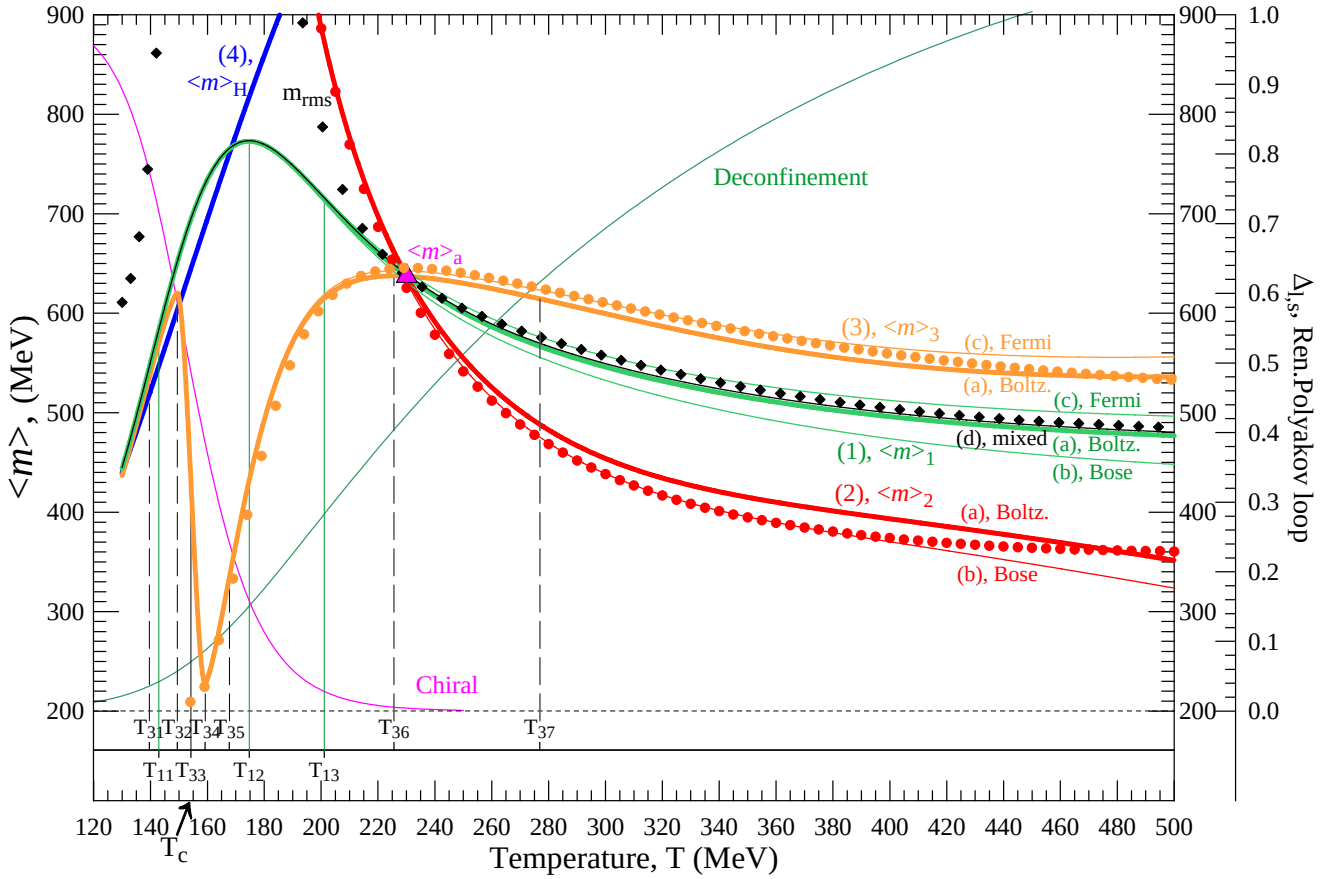


Figure 5: The average mass $\langle m \rangle$ calculated through method 1 with $\Delta T = 5$ MeV. Curves (1), $\langle m \rangle_1$, correspond to system 1, curves (2), $\langle m \rangle_2$, to system 2, curves (3), $\langle m \rangle_3$, to system 3 and curve (4), $\langle m \rangle_H$, to HRG. Thick lines (a) are calculated with the Boltzmann approximation, lines (b) with Bose statistics, lines (c) with Fermi statistics and thin continuous line (d) to a system composed of $\frac{16}{52}$ bosons and of $\frac{36}{52}$ fermions. Solid rectangles represent the value of m_{rms} calculated through the values of lines (2a) and (3a) of this figure and figure 4 and are compared with line (1a). Solid triangle represents a point with common solution for average mass, $\langle m \rangle_a$, for all systems, 2, 3 and 1. The order parameters of the chiral transition and deconfinement are shown, as in Fig. 1. The shown characteristic temperatures $T_{31...36}$, $T_{11...13}$ are defined in Fig. 6 and Table 2. With solid circles we present the calculations of $\langle m \rangle$ in the Boltzmann approximation for systems 2 and 3 carried out with the Lattice results from [7].

8.6%. Also, the Fermi statistics for system 3 and the fitting function of eq. (35) for system 1 drive the results of g_t closer to the values g_Q and q_T, respectively.

In Figure 4 we have also plotted the value of the sum $g_{t,g} + g_{t,q}$ for the Boltzmann calculations (solid triangles). This value almost coincides with the value for the total system $g_{t,1} \simeq g_{t,2} + g_{t,3}$, for temperatures $T > 210$ MeV. The situation is similar to the simple system of figure 2(i) (temperature is high enough so both particle species are present in the effective description). On the contrary, $g_{t,1}$ departs from the sum $g_{t,2} + g_{t,3}$ in the region 145 MeV$< T <$ 210 MeV, acquiring considerably less value than this sum. This is due to the high average mass of system 2. Thus, in this region $g_{t,1}$ is closer to $g_{t,3}$.

In Figure 5 we present the calculation of m_{rms} (solid rectangles) for a system which is composed of quarks and gluons:

$$m_{rms} = \sqrt{\frac{g_{t,2} \langle m \rangle_2^2 + g_{t,3} \langle m \rangle_3^2}{g_{t,2} + g_{t,3}}} \ . \tag{36}$$

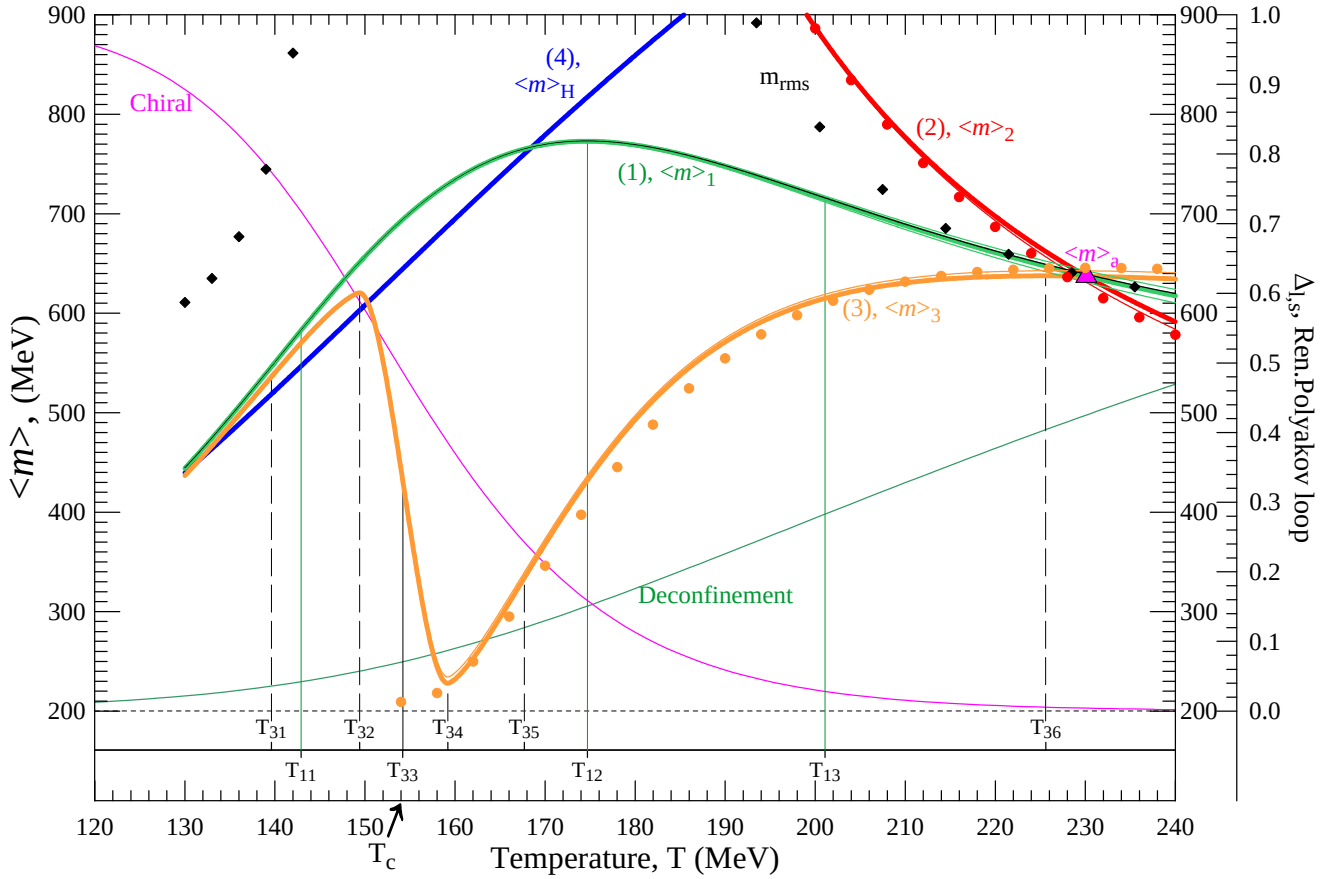


Figure 5a: Fig. 5 focused on the temperature range 120-240 MeV.

This value is very close to average mass of system 1 $\langle m \rangle_1 \simeq m_{rms}$ for temperatures $T > 210$ MeV, situation similar to the simple system of figure 2(ii).

It is also seen that at a certain temperature $T_a \simeq 230$ MeV all systems, 3, 2 and as a consequence 1, obtain the same average mass $\langle m \rangle_a \simeq 637$ MeV. This means that at this temperature all systems can be described with the same common effective mass. This mass appears indicated with a solid triangle in Figure 5.

We found that at high temperatures the quark states approximately lock onto their value of degrees of freedom that correspond to the free system, but with considerably high average mass. It would be interesting to seek the values of masses which correspond to each of the two quark species (u and d quarks are considered identical and are denoted as q) at this high temperature limit. For this reason we have performed a calculation at T =500 MeV. We use the pressure P_3 and entropy density s_3 at this temperature, according to eqs. (5). We fix by hand the number of states for the q-quarks at 24 and for the s-quarks at 12. Subsequently we use the Fermi statistics and leave as parameters to be determined two different mass terms $\langle m \rangle_q$ and $\langle m \rangle_s$ for the two kinds of quarks. The result of the fit is $\langle m \rangle_q \simeq$482 MeV and $\langle m \rangle_s \simeq$716 MeV, which correspond to $\langle m \rangle_{rms} \simeq$571 MeV. The last value can be compared with the value one can find if only one mass parameter is used for all the quarks (with g_{t3} =36): $\langle m \rangle \simeq$563 MeV (close to the $\langle m \rangle_{rms}$ value).

The calculated $\langle m \rangle_q$ and $\langle m \rangle_s$ are still well above the current quark masses ∼3.5 MeV and ∼98 MeV, as well as above the constituent quark masses ∼338 MeV and ∼486 MeV. This suggests that the quarks are still in interaction with the gluonic field at T=500 MeV.

Recently, new Lattice calculations for the pure SU(3) pressure and entropy density have been carried out [7]. We have carried out the calculations for g_t and $\langle m \rangle$ for systems 2 and 3 with method

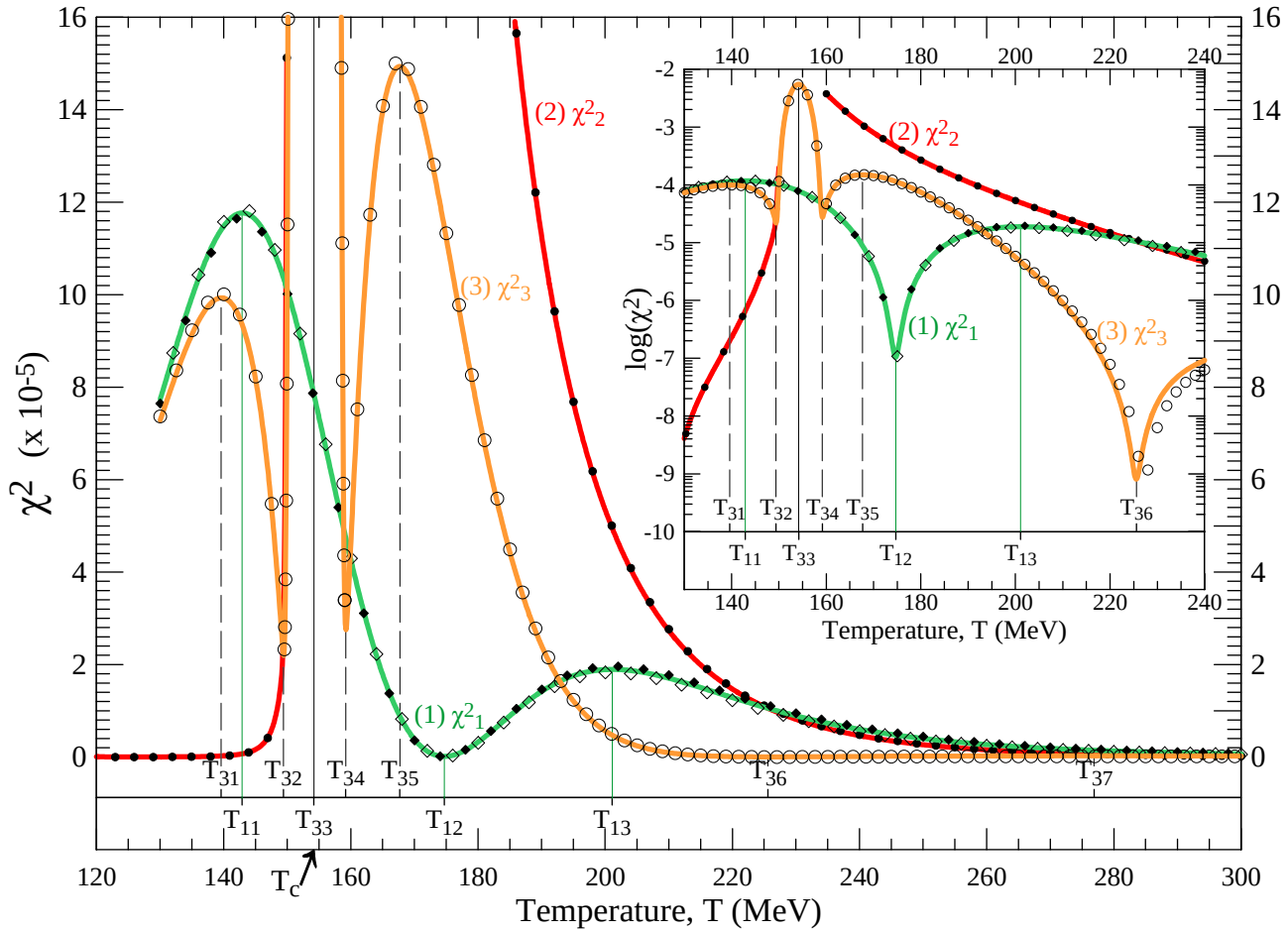


Figure 6: The value of χ^2 which results from the fit to determine the parameters g_t and $\langle m \rangle$ through method 1 with $\Delta T = 5$ MeV in linear and logarithmic vertical axis (embedded graph). Curve (1), χ^2_1, corresponds to system 1, curve (2), χ^2_2, to system 2 and curve (3), χ^2_3, to system 3. Thick lines are calculated with the Boltzmann approximation, while solid dots represent the use of Bose statistics for system 2 and open circles the use of Fermi statistics for system 3. For system 1, temperatures T_{11} and T_{13} represent location of maximum values of χ^2 and T_{12} corresponds to minimum value. For system 3, temperatures T_{31}, T_{33}, T_{35} and T_{37} represent location of maximum values of χ^2 and T_{32}, T_{34}, T_{36} correspond to minimum values. See also Table 2.

T (MeV)	Label	System	Extremal of χ^2	Extremal of g_t, $\langle m \rangle$
139.6	T_{31}	3	max	-
142.9	T_{11}	1	max	-
149.4	T_{32}	3	min	max
154.2	T_{33}	3	max	-
159.2	T_{34}	3	min	min
167.7	T_{35}	3	max	-
174.7	T_{12}	1	min	max
201.1	T_{13}	1	max	-
225.6	T_{36}	3	min	min
276.9	T_{37}	3	max	-

Table 2: Location of the extremal points of χ^2 for systems 1 and 3, as well as, their connection with the fitted parameters of Figures 4 and 5. The maxima of χ^2 depend on the choice of the errors σ, while the minima remain unchanged. In this calculation we have used $\sigma = T^4$.

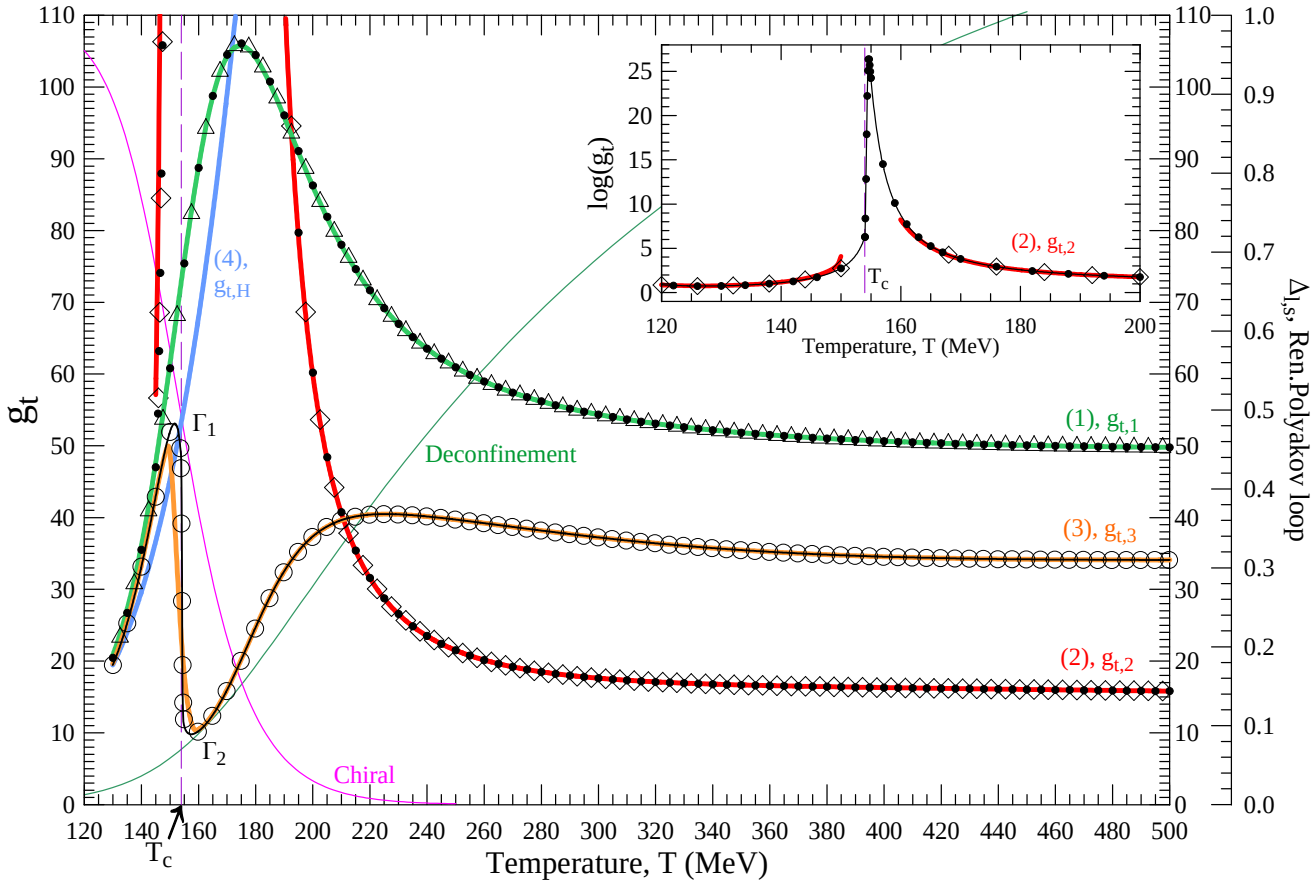


Figure 7: The effect of the methodology of calculation on the number of states, g_t. All calculations in this graph have been carried out in the Boltzmann approximation. Curves (1), $g_{t,1}$, correspond to system 1, curves (2), $g_{t,2}$, to system 2, curves (3), $g_{t,3}$, to system 3 and curve (4), $g_{t,H}$, to HRG. Thick continuous lines are calculated through method 1 with $\Delta T = 5$ MeV. Solid points near line (1) and (2) and solid dark line near line (3) are the calculations through method 2 for system 1, 2 and 3, respectively. Open symbols represent calculations through method 1 with $\Delta T = 0.5$ MeV (triangles for system 1, rectangles for system 2 and circles for system 3). The order parameters of the chiral transition and deconfinement are shown, as in Fig. 1. Points Γ_1 and Γ_2 show regions of results sensitive to the methodology of calculation we used. The embedded graph with the logarithmic vertical axis focuses on the calculations of system 2 around critical temperature T_c.

1 in the Boltzmann approximation, which are depicted in Figs. 4 and 5, respectively. The extracted parameters exhibit, apart from small variations with respect to the use of [5], the same overall behaviour. This finding contributes to the stability and consistency of our description.

In Figure 6 we examine the shape of χ^2 as function of temperature for system 1 (curve (1)), system 2 (line (2)) and system 3 (line (3)). For the error σ we have used the function (12). The temperatures where the local maximum values of χ^2 are located, represent transition points from one effective description with g_t and $\langle m \rangle$ to another, as discussed in the method section. The minimum values of χ^2, on the contrary, correspond to conditions where the relatively best description is achieved. It is found that the minimum values of χ^2 coincide with local maxima or minima of g_t and simultaneously $\langle m \rangle$ with respect to temperature. The minima of χ^2 remain practically unchanged under different choices of the errors σ. We have checked the validity of this fact with the choices $\sigma = const.$, $\sigma = T^4$ and $\sigma = P_L(T)$. The location of the maxima of χ^2, however, depend on the choice of the function used for the σ, but the existence of two successive

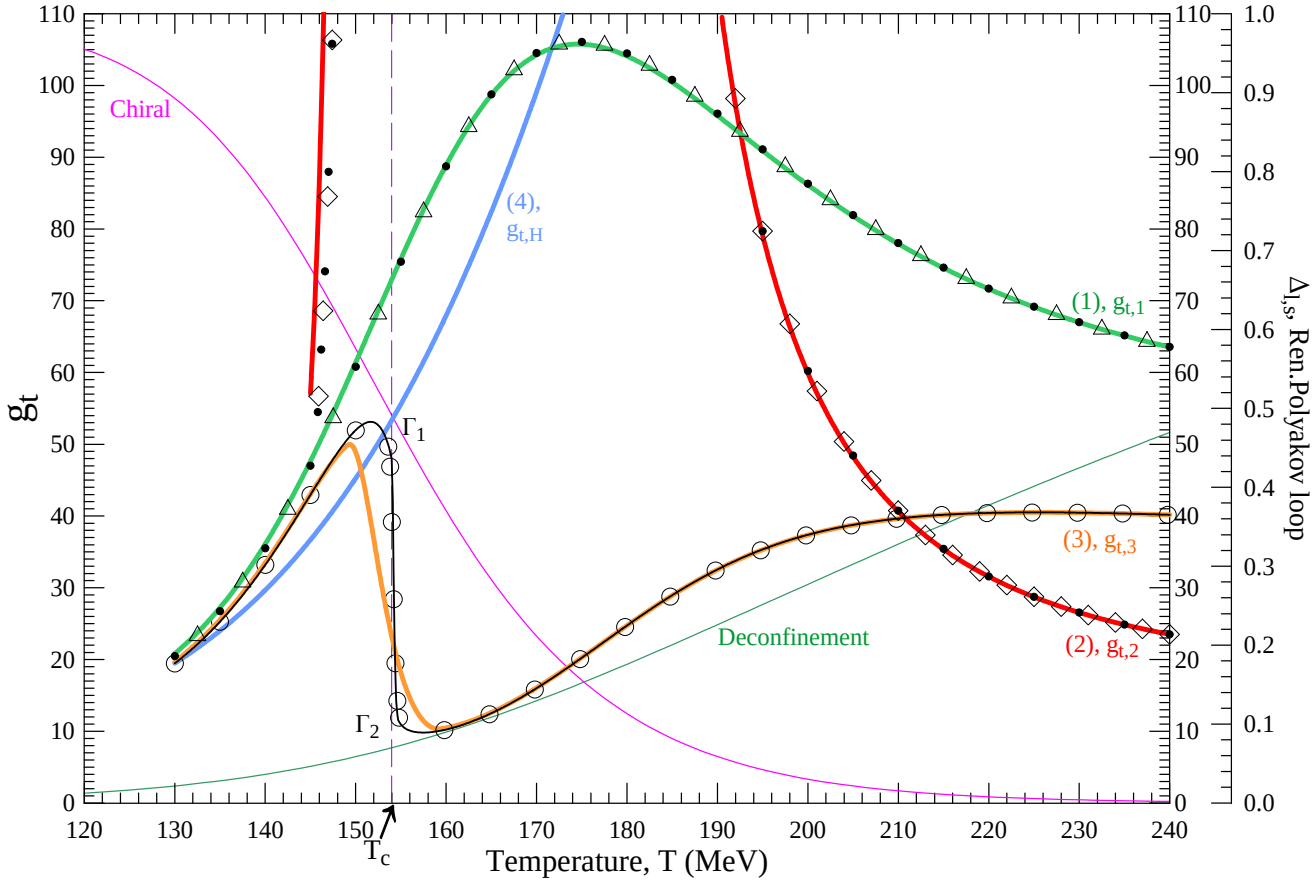


Figure 7a: Fig. 7 focused on the temperature range 120-240 MeV.

stable minima will always lock the position of the corresponding maximum between them. For system 1 two maximum values are found at T_{11} and T_{13} and one minimum at T_{12}. For system 2, method 1 fails to produce results in the region 150 MeV $< T <$ 160 MeV. However, as it is evident from Figure 6, an extreme maximum is formed in this region. For system 3 there are four maxima at T_{31}, T_{33}, T_{35} and T_{37}. The highest maximum is located at T_{33}, which is close to the transition temperature T_c. There are also three minima, at T_{32}, T_{34} and T_{36}. The minimum at T_{36} is very close to temperature T_a discussed above. The positions of the local extremal of χ^2 for systems 1 and 3 are listed in Table 2. These characteristic temperatures are, also, depicted in Figs. 4 and 5. From these two graphs it is deduced that the minimum values of χ^2 coincide with local maxima or minima of g_t and simultaneously $\langle m \rangle$ with respect to temperature.

The value of χ^2 can also reveal the quality of the fit. In order to estimate the value of χ^2 to be used for this purpose we have to use for the errors σ in eq. 11 a value comparable to the sum $\sum_{i=1}^{N} [P_L(T_i) - P_f(T_i)]^2$. One suitable choice is $\sigma' = 0.1 P_L(T)$, where T is the central temperature in the aforementioned sum and the value 0.1 corresponds to a typical relative experimental error. The value of χ^2 also needs to be divided to the corresponding degrees of freedom (dof) which are 99 (101 data points minus 2 fitted parameters). The quality of the fit may then be estimated by the quantity

$$\frac{\chi'^2}{dof} = \frac{\chi^2}{dof} \left[\frac{\sigma}{0.1 P_L(T)} \right]^2 . \tag{37}$$

If we exclude system 2 around the critical temperature T_c, it is seen that the highest value of χ^2 for all systems corresponds to system 3 near T_c (see fig. 6). For this value of $\chi^2 = 5.51 \cdot 10^{-3}$ we calculate $\frac{\chi'^2}{dof} = 1.15 \cdot 10^{-4}$. The value of $\frac{\chi'^2}{dof}$ is considerably lower for the rest of the temperatures.

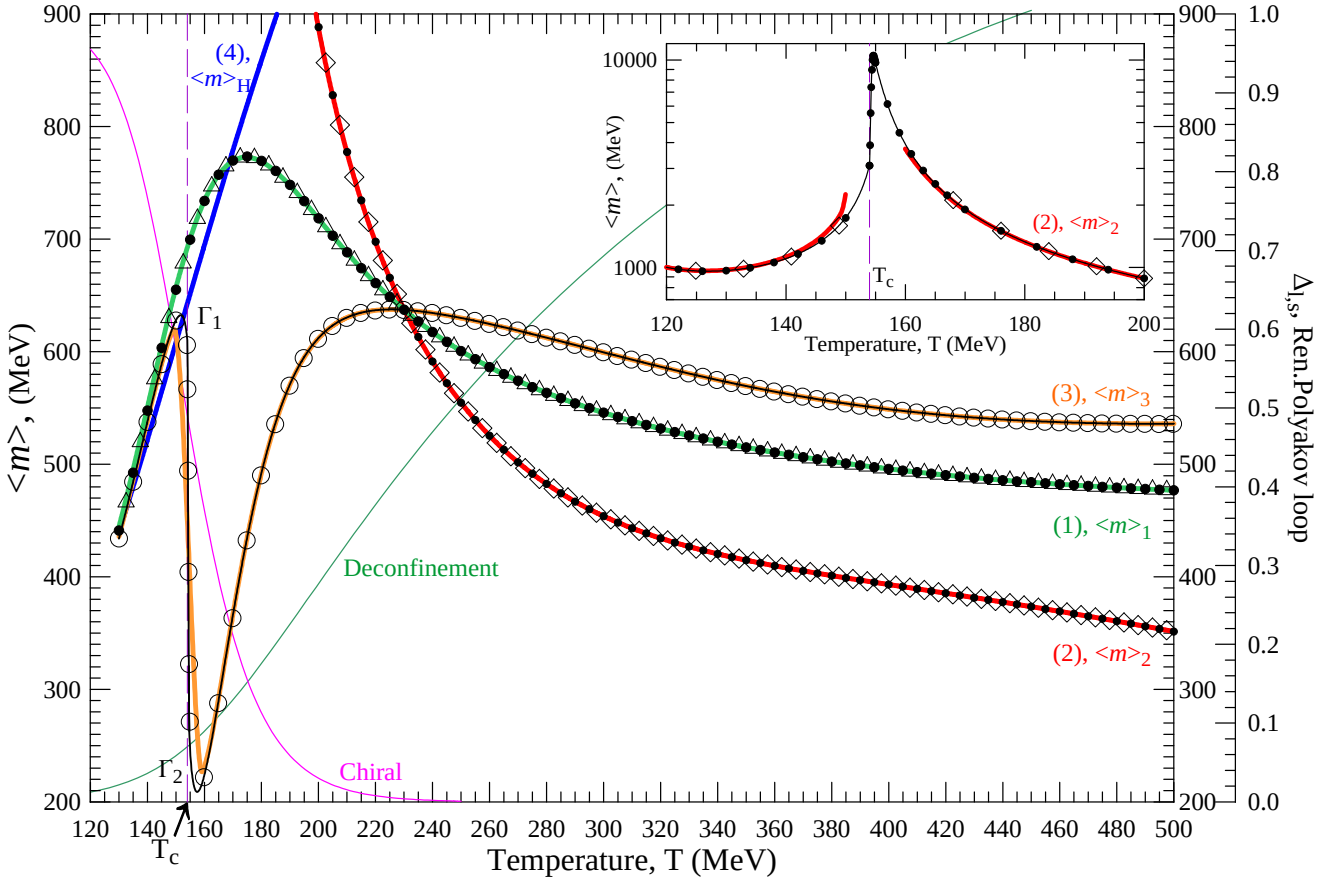


Figure 8: The effect of the methodology of calculation on the average mass, $\langle m \rangle$. All calculations in this graph have been carried out in the Boltzmann approximation. Curves (1), $\langle m \rangle_1$, correspond to system 1, curves (2), $\langle m \rangle_2$, to system 2, curves (3), $\langle m \rangle_3$, to system 3 and curve (4), $\langle m \rangle_H$, to HRG. Thick continuous lines are calculated through method 1 with $\Delta T = 5$ MeV. Solid points near line (1) and (2) and solid dark line near line (3) are the calculations through method 2 for system 1, 2 and 3, respectively. Open symbols represent calculations through method 1 with $\Delta T = 0.5$ MeV (triangles for system 1, rectangles for system 2 and circles for system 3). The order parameters of the chiral transition and deconfinement are shown, as in Fig. 1. Points Γ_1 and Γ_2 show regions of results sensitive to the used methodology of calculation. The embedded graph with the logarithmic vertical axis focuses on the calculations of system 2 around critical temperature T_c.

Thus, we conclude that we have a successful effective description for all systems in all temperatures, with the exception of system 2 in the vicinity of T_c.

We investigate further the stability of χ^2 under the influence of change of the statistics. In Figure 6 we have plotted the evaluation of χ^2 for system 2 with the use of Bose statistics (solid points) and for system 3 with Fermi statistics (empty circles). No apparent change is found (with the exception of the small shift of the minimum T_{36}), proving that χ^2 remains practically unaltered by the change of the type of statistics used.

In the following we inspect the influence on our results of changing ΔT in method 1 (the temperature interval around the central temperature T on which we impose our fits), as well as using method 2, instead of method 1. In Figures 7 and 8 we show results for g_t and $\langle m \rangle$, respectively. We have plotted by thick continuous lines the results of method 1 with ΔT=5 MeV. The results of method 2 are plotted by solid points for systems 1 and 2 and by thin continuous line for system 3. The results of method 1 with ΔT reduced to 0.5 MeV are shown with open symbols, triangles for system 1, rectangles for system 2 and circles for system 3. We find complete stability of our results

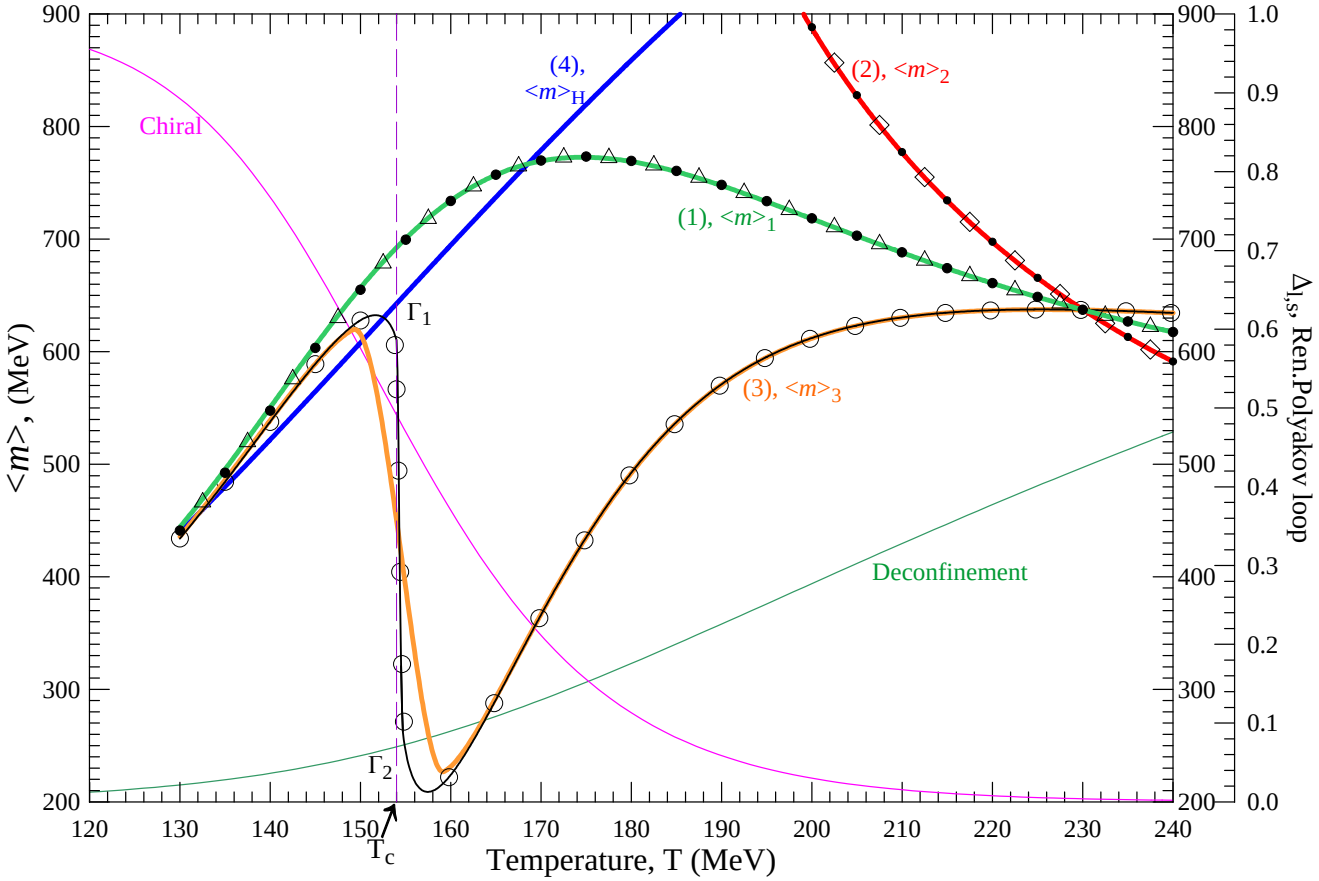


Figure 8a: Fig. 8 focused on the temperature range 120-240 MeV.

in the whole temperature range of our analysis under changing of the method or the magnitude of ΔT. The only exception appears in the abrupt variation of g_t and $\langle m \rangle$ in the case of system 3 (see points Γ_1 and Γ_2) around the critical temperature T_c. The reduction of the temperature interval ΔT or the use of method 2 leads to a steepest descend of our fitted parameters with temperature increase. The equivalence of method 2 with the reduction of ΔT is expected, since method 2 is identical to method 1 for ΔT=0.

In Figures 7 and 8 we have embedded a figure to show the behaviour of system 2 in the temperature interval (150-160) MeV. Method 1 fails at this region, but method 2 is able to produce results, which are shown in the graph. The extreme rise of the parameters g_t and $\langle m \rangle$ occurs around the critical temperature T_c. The exact values of the parameters are not trustworthy in this region. The reason is that we have used the smoothing interpolating function 4 and that χ^2 of method 1 is forming an extreme maximum as can be seen in Fig. 6. However, it indicates qualitatively an extreme increase of the number of states and the effective mass of the gluons around the critical temperature. The emerging picture is as if the gauge field occupies the whole system as a unique entity. This system, around the critical temperature, cannot be described as a group of "particles" with specific mass and states, since the interaction is such that the whole system behaves as a single "particle" with divergent mass and number of states.

Finally, in Figure 9 we check the effect on χ^2 of changing ΔT in method 1. In this Figure we present the calculations for $\Delta T = 5$ MeV (lines (i), upper) and $\Delta T = 0.5$ MeV (lines (ii), low). We find that χ^2 is decreasing as ΔT reduces. This is expected, since in method 2 we have identically $\chi^2 = 0$ (two parameters are determined through solving two equations) and also $\Delta T = 0$. Thus, we expect that the reduction of ΔT causes χ^2 to decrease, since both of these non-negative

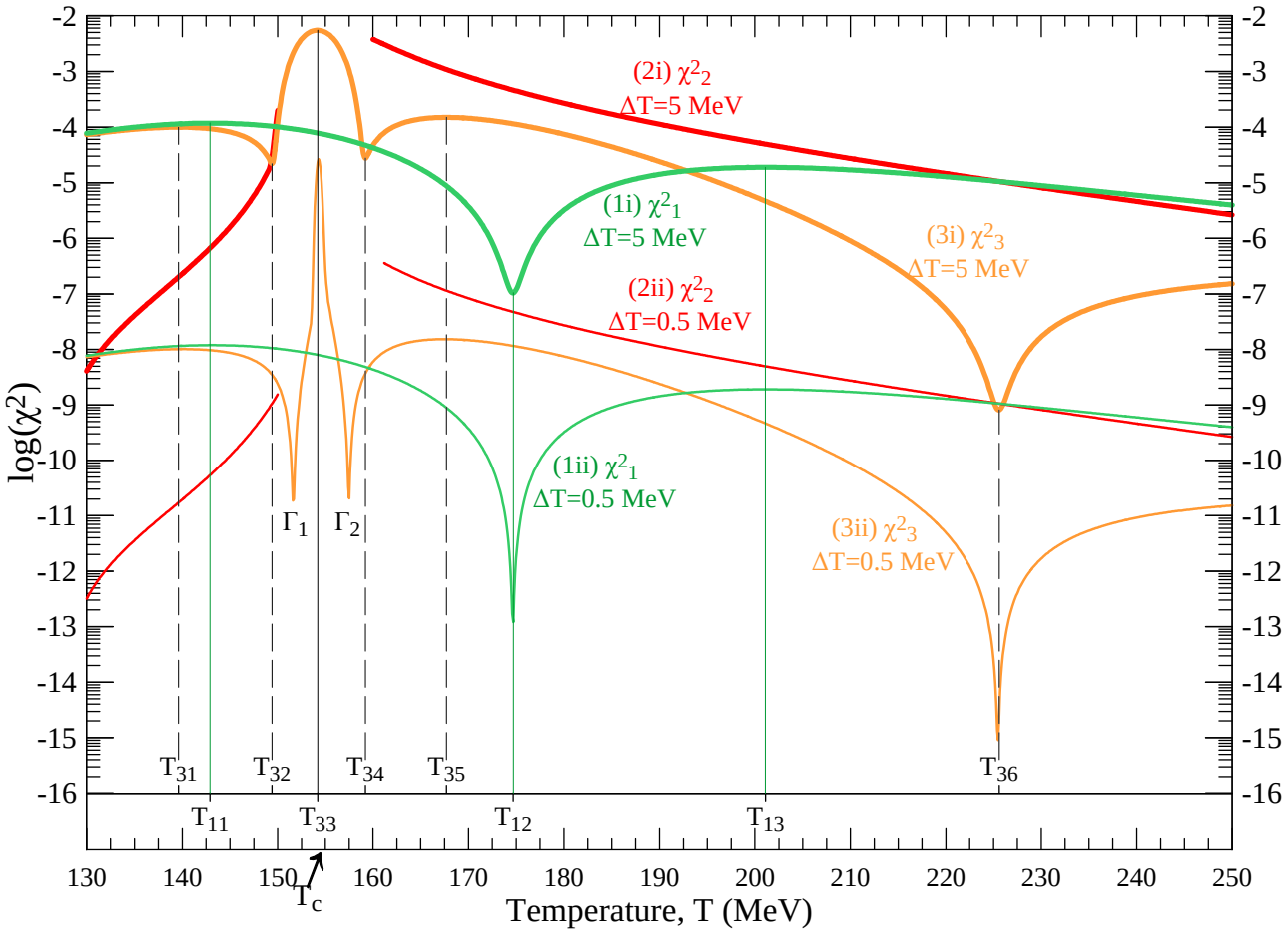


Figure 9: The effect of the methodology of calculation on the value of χ^2. The calculations have been carried out in the Boltzmann approximation. Upper, thick curves (i) represent calculations through method 1 with $\Delta T = 5$ MeV, while low, thin curves (ii) represent calculations through method 1 with $\Delta T = 0.5$ MeV. Curves (1), χ^2_1, correspond to system 1, curves (2), χ^2_2, to system 2 and curves (3), χ^2_3, to system 3. The shown characteristic temperatures are the same as in Figure 6 and are all stable under change of ΔT, except for T_{32} and T_{34}.

quantities should approach the zero limit. The figure shows that the extremal points of χ^2 remain unchanged under variation of ΔT. The only exception appears to the minima T_{32} and T_{34} of system 3. Reduction of ΔT causes both of them to approach the location T_{33} of the corresponding maximum of χ^2. The behaviour is consistent with figures 7 and 8, where the reduction of ΔT leads to steepest variation of g_t and $\langle m \rangle$ around T_c. Consequently, this leads to narrowing the gap between the location of maximum and minimum values of these parameters.

5 Concluding Remarks

We have developed an effective description of the Lattice QCD pressure and specific entropy at zero baryon chemical potential with two parameters, the degeneracy factor, g_t and the average particle mass $\langle m \rangle$. The description is carried out for the three flavour QCD system (system 1), as well as the pure gauge field (system 2) and a system containing quarks in interaction with gluons (system 3).

The calculated parameters of systems 1 and 3 have as their low temperature limit the corresponding parameters of the Hadron Resonance Gas. The number of states for all systems (1, 2 and

3) converge, above $T \simeq 230$ MeV, close to the number of states of an ideal Quark-Gluon Phase, indicating the existence of colour states at these temperatures. The corresponding high average masses, though, suggest that the entities are strongly interacting.

The number of states and the average mass, corresponding to system 2, are found to be in extreme increase just below the critical temperature, T_c and in extreme decrease just above T_c.

Between $T \simeq 150$ and 160 MeV the average mass and the number of states corresponding to system 3 are found to decrease steeply, deviating from the HRG parameters. However, the minimum value of degrees of freedom at this temperature interval indicates the existence of hadronic states. One possible explanation of this behaviour would be the reduction of the available hadron resonances and their limitation to a few states. Between 160 MeV and ~ 220 MeV the number of states is increasing approaching an almost constant value, equal to that of a system of three flavour, coloured quark states. The described changes of systems 3 and 2 are taking place within the temperature range of the chiral transition.

The value of χ^2 which results after the optimization of the parameters g_t and $\langle m \rangle$ can be used as a tool to locate regions of relatively best effective descriptions in terms of these parameters, as well as points of transition between them. The low values of this quantity, after proper normalization, ascertains the success of the description with the fitted parameters.

Acknowledgement. We wish to thank N. G. Antoniou and F. K. Diakonos for useful suggestions and fruitful discussions.

References

[1] R. Hagedorn, "Thermodynamics of Strong Interactions", Lectures Given in the Academic Training Programme of CERN 1970-71, CERN 71-12, 7 May 1971

[2] E.P. Politis, C.E. Tsagkarakis, F.K. Diakonos, X.N. Maintas and A. Tsapalis, Phys. Lett. B **763** (2016) 139.

[3] A. Bazavov et. al., (HotQCD Collaboration), Phys. Rev. D **90** (2014) 094503; arXiv:1407.6387 [hep-lat].

[4] J. Cleymans, H. Satz, Z. Phys. C **57** (1993) 135; J. Letessier, A. Tounsi, J. Rafelski, Phys. Lett. B **292** (1992) 417; J. Letessier, A. Tounsi, U. Heinz, J. Sollfrank, J. Rafelski, Phys. Rev. D **51** (1995) 3408; F. Becattini, M. Gaździcki, A. Keränen, J. Manninen, R. Stock, Phys. Rev. C **69** (2004) 024905; J. Cleymans, K. Redlich, Phys. Rev. Lett. **81** (1998) 5284.

[5] Sz. Borsányi, G. Endrődi, Z. Fodor, S.D. Katz and K.K. Szabó, JHEP **1207** (2012) 056; arXiv:1204.6184 [hep-lat].

[6] Sz. Borsányi, Z. Fodor, C. Hoelbling, S.D. Katz, S. Krieg, C. Ratti and K.K. Szabó, JHEP **2010** (2010) 73; arXiv:1005.3508 [hep-lat].

[7] L. Giusti and M. Pepec, Phys. Lett. B **769** (2017) 365; arXiv:1612.00265 [hep-lat].